

**Spermiogenesis and biflagellate spermatozoon
of the teleost fish *Lampanyctus crocodilus* (Myctophiformes, Myctophidae):
ultrastructure and characterization of its sperm basic nuclear proteins**

E. Ribes, M. Cheema, R. González-Romero, D. Lloris, J. Ausió, N. Saperas*

Enric Ribes

Departament de Biologia Cel·lular, Facultat de Biologia, Universitat de Barcelona, Av. Diagonal
645, 08028 Barcelona, Spain

Manjinder Cheema, Rodrigo González-Romero, Juan Ausió

Department of Biochemistry and Microbiology, University of Victoria, British Columbia, Canada
V8W 3P6.

Domingo Lloris

Departament de Recursos Marins Renovables, Institut de Ciències del Mar (CSIC), Pg. Marítim de
la Barceloneta, 37-49, 08003 Barcelona

Núria Saperas*

Departament d'Enginyeria Química, ETSEIB, Universitat Politècnica de Catalunya, Av. Diagonal
647, 08028 Barcelona, Spain

e-mail: nuria.saperas@upc.edu

(*) Corresponding author

Keywords:

Lampanyctus, myctophiformes, biflagellate sperm, fish spermiogenesis, sperm
nuclear basic proteins

Abstract

In this work we provide the ultrastructural study of the spermiogenesis of the lanternfish *Lampanyctus crocodilus* (Myctophiformes, Myctophidae) with special emphasis on the condensation of chromatin and the biochemical characterization of its sperm nuclear basic proteins (SNBPs). The round head of the early spermatid of *L. crocodilus* develops into a curved conical-shaped head in the spermatozoon. Two flagella, already present in the spermatid, are inserted laterally at the convex side of the sperm head. Both flagella possess a 9+0 axoneme instead of the typical 9+2 axonemal structure. Mitochondria undergo a characteristic redistribution during spermiogenesis. A reduced number of them are present away from the centrioles at both ends of the concave side of the sperm head. In the process of chromatin condensation during spermiogenesis, fibrogranular structures with granules of 25 ± 5 nm and 50 ± 5 nm can be observed in the early spermatid, which develop into larger granules of about 150 ± 50 nm in the middle spermatid. They later coalesce during the transition to advanced spermatid and spermatozoon giving rise to a highly condensed chromatin organization in the sperm cell. Protamines are the main SNBPs associated with this chromatin; however, they are unusually large and correspond to the largest protamines described in fish to date. Small stoichiometric amounts of histones as well as other basic proteins coexist with these protamines in the spermatozoon.

Introduction

Spermiogenesis and spermatozoa ultrastructure has been studied in many fish species (see the reviews by Jamieson 1991, 2009a; Mattei 1991b; Lahnsteiner and Patzner 2007; and references therein). However, in some groups of fishes, such as the Myctophiformes, very little information is available (Jamieson 2009b).

The teleost fish *Lampanyctus crocodilus* (Risso 1810) belongs to the family Myctophidae (lanternfishes), which is the most abundant of the two families in the order Myctophiformes (Myctophidae and Neoscopelidae). About 32 genera with at least 240 species are included in this family (Nelson 2006). They are deep-sea marine fishes that can be found in all oceans. The name lanternfish refers to their ability to produce bioluminescence through a number of photophores distributed along their body (Hulley 1984).

A brief ultrastructural report on the spermatid and spermatozoon of *Lampanyctus* sp was provided by Mattei and Mattei (1976). According to these authors, the spermatozoon has an S-shaped completely opaque nucleus and an acrosome is lacking (as is characteristic of the neopterygian fishes) (Jamieson 1991). They described the early spermatid and the spermatozoon as biflagellate cells with a 9+0 axonemal structure and pointed out that this was the only known fish where biflagellarity and the 9+0 pattern coexisted. These characters were later found in two more members of the family Myctophidae: *Symbolophorus californiensis* and *Notoscopelus* sp. (Hara 2007). However, contrary to these observations, Hara and Okiyama (1998) report that in *Lampanyctus jordani* the spermatozoon has a spherical head, is uniflagellated, and with a 9+2 axonemal structure (reviewed in Jamieson 2009b). This variability in the same genus is certainly surprising and the

study of more species is needed to reach a more general view. Also, a detailed ultrastructural study of the spermiogenic process is missing.

One of the most dramatic changes occurring during spermiogenesis is the remodelling of the sperm chromatin. The proteins that organize DNA in the sperm nuclei are usually called SNBPs (sperm nuclear basic proteins). In contrast to the proteins associated with somatic chromatin (somatic histones), SNBPs exhibit a great variability. However, they can be classified in three main groups: the histone type (H type), the protamine-like type (PL type) and the protamine type (P type) (reviewed in Ausió 1999; Eirín-López and Ausió 2009). The H type includes proteins compositionally and structurally related to somatic histones. The P type encompasses a group of small arginine-rich highly basic proteins which usually replace the majority of the germinal somatic-like histones, achieving a higher degree of chromatin condensation. Finally, the PL type includes a group of proteins that are structurally and functionally intermediate between the H and the P type, and which are related to histone H1. Although the P type is prevalent among teleost fishes, examples of the other two types can also be found (Saperas et al. 1993a; Saperas et al. 1994; Frehlick et al. 2006).

In the present work we have been able to obtain fresh mature specimens of *Lampanyctus crocodilus* and provide an ultrastructural characterization of the spermiogenesis of this species. We have also studied the chromatin condensation pattern, and we give a biochemical characterization of the sperm nuclear basic proteins associated with the chromatin of this spermatozoon.

Materials and methods

Animals

Specimens of *Lampanyctus crocodilus* (Jewel lanternfish) (Myctophidae, Myctophiformes) were collected from the Mediterranean Sea (Barcelona, Catalonia, Spain) during April and May. Upon collection, they were maintained on ice until arrival to the shore destination where they were dissected right away. Flowing sperm samples were obtained by gentle abdominal massage. Testes were checked by bright field or phase microscopy and only ripe gonads containing sperm cells were used.

Testis and sperm samples intended for the ultrastructural studies were immediately fixed as described below. Samples to be used in biochemical analysis were preserved in 90% ethanol at -20°C until further processing (see below).

Transmission electron microscopy (TEM)

Fresh testes samples were fixed for 3 hours at 4°C in 2% paraformaldehyde - 2.5% glutaraldehyde mixture in 0.1 M cacodylate buffer (pH 7.2), with 0.1 M sucrose and 0.2 mM calcium chloride. They were post-fixed for 1 hour at 4°C in 2% osmium tetroxide in the same buffer, followed by acetone dehydration and embedding in Spurr's resin. Ultrathin sections were obtained on an ultramicrotome (Leica Ultracut UCT), stained with uranyl acetate and lead citrate, and then examined with a Jeol EM-1010 electron microscope operating at 80 kV.

Scanning electron microscopy (SEM)

Fresh sperm and testes samples were minced and dispersed in PBS and the resulting cell suspensions were glued on poly-L-lysine-coated coverslips. These samples were fixed (2 hours) and post-fixed (2 hours) at 4°C as in TEM, and dehydrated using a series of increasing ethanol for 30 minutes. The samples were next dried at their critical point with carbon dioxide and sputter coated with gold-palladium. Analysis was carried out on a Jeol J-6510 scanning electron microscope at 10 -15 kV acceleration voltage.

Extraction and purification of sperm basic nuclear proteins (SNBPs)

Nuclei were prepared as previously described (Saperas et al. 1993a) with slight modifications. Briefly, ripe male gonads were homogenized in a Dounce in 4-5 volumes of ice-cold buffer A [0.25 M sucrose, 5 mM CaCl₂, 50 mM Tris-HCl (pH 7.4)], containing 50 mM benzamidine chloride as a protease inhibitor (Chiva et al. 1988), filtered and centrifuged (2300xg, 10 min, 4°C). Pellets were homogenized with buffer A containing 0.1% Triton X-100 and centrifuged under the same conditions. This step was repeated one more time. Before protein extraction, pellets were homogenized in ice-cold buffer B [20 mM EDTA, 50 mM Tris-HCl (pH 7.4)], centrifuged, and then homogenized in ice-cold buffer C [50 mM Tris-HCl (pH 7.4)] and centrifuged one last time. In those instances where sperm or gonad from a single specimen was processed, the homogenization steps with buffers B and C were omitted and all the steps were carried out in an Eppendorf tube.

SNBPs were extracted from the nuclear pellets with 0.4 N HCl. In some instances, a sequential acid solubilisation of the SNBPs was performed. In these instances, a first extraction was carried out with 35% acetic acid in order to solubilise the histone component (Chiva et al. 1992). After centrifuging at 16,000xg, HCl was added to the supernatant to make it 0.25 N HCl and the pellet was re-extracted right away with 0.4 N HCl and centrifuged again to recover the supernatant. Proteins from all the acid extracts were immediately precipitated overnight with 6 volumes of acetone at -20°C . The protein precipitates were recovered by centrifugation at 16,000xg, rinsed with cold acetone and finally dried (Chiva et al. 1990).

Protein fractionation and purification was performed by either reversed phase high performance liquid chromatography (RP-HPLC) or by cationic exchange fast performance liquid chromatography (FPLC). RP-HPLC was performed using a Vydac C₁₈ 4.6 x 250 mm column eluted with acetonitrile gradients in the presence of trifluoroacetic acid (TFA) (as indicated in the figures). Two solutions were used for the generation of the gradients: solution A (0.1% TFA) and solution B (100% acetonitrile), as described elsewhere (Ausió 1988). Cationic exchange chromatography was carried out on an ÄKTA Purifier 10 FPLC system using a HiTrap SP FF column (GE Healthcare). Elution was carried out with a gradient from 50 mM to 2 M NaCl in 50 mM sodium acetate (pH 6.0). Some of the fractions obtained in this way were dialysed, lyophilized and re-fractionated by HPLC as described above.

Electrophoretic analyses

Acetic acid/urea polyacrylamide gel electrophoresis (AU-PAGE) was carried out as described elsewhere (Saperas et al. 1992). For the two-dimensional gel electrophoresis (2D-PAGE), AU-PAGE was used for the first dimension and sodium dodecyl sulfate polyacrylamide gel electrophoresis (SDS-PAGE) (Laemmli 1970) was used for the second dimension. Slices of the lanes from the AU-PAGE were soaked for 20 minutes in the stacking SDS gel solution [6% acrylamide, 0.16% bisacrylamide, 0.125 M Tris (pH 6.8), 0.1% SDS] under constant shaking prior to loading on top of the SDS gel.

Mass spectrometry and amino acid analysis

Matrix-assisted laser desorption/ionization (MALDI) was carried out as described previously (Hunt et al. 1996). Amino acid analysis was carried out as in Kasinsky et al. (2005).

Results

During *L. crocodilus* spermiogenesis, round spermatids develop into a biflagellate sperm cell with modified head morphology (Fig. 1). The two flagella, already present in the spermatid phases, will grow to reach a final length of about 55 μm (Fig. 1a, c).

Ultrastructure of the spermatid

The early spermatid of *L. crocodilus* is a round cell with a voluminous nucleus in a central position, surrounded by a number of mitochondria which are very close to the nuclear envelope. Dispersed flat cisternae of endoplasmic reticulum (ER) can also be seen in the cytoplasm (Fig. 2a, b). A pair of centrioles is found in the basal pole of the cell and they give rise to a pair of flagella that will develop during this stage (Fig. 1b). The nuclear envelope membranes of this region are in intimate contact and present higher electron density than in the rest of the nucleus (Fig. 2b). A dense fibrous pericentriolar structure is found associated with both the centrioles and the nuclear envelope (arrowheads in Fig. 2b).

From the early stages of spermiogenesis, a high number of non-electron dense vesicles are found in the cytoplasm (Fig. 2c). These vesicles together with other cytoplasmic material are removed from the cell as cytoplasmic drops (arrows in Fig. 2c). These residual bodies are observed around the spermatid in the lumen of the spermatogenic tubules. They will be phagocytosed by the Sertoli cells found next to the peritubular myoid cells of the walls of these tubules (Fig. 2d).

The middle spermatid is also a round cell but with a slightly reduced volume. At this stage, mitochondria have diminished in number and they are not found uniformly distributed around the nucleus anymore, but grouped in a position distant from the basal pole of the cell and close to the nuclear envelope (Fig. 2e). The nucleus loses its spherical shape in the apical pole, opposite to the centrioles. Its conformation flattens and undergoes a transition to a semi-spherical shape (Fig. 2e, g)

At this stage, the fibrous pericentriolar structure that is observed in the early spermatid (Fig. 2b) undergoes a substantial enlargement and adopts a concave shape that surrounds the basal region of the nucleus and is associated with the centrioles (Fig. 2f).

The advanced spermatid of *L. crocodilus* undergoes a dramatic change both in its internal and external morphology, and transforms from a rounded cell to a curved conical shaped cell. At the beginning of this transition, the cytoplasm from the spermatid apical zone invaginates to the interior of the nucleus, which adopts a “C” shape and exhibits an internal concave side and an external convex side (Fig. 3a). The mitochondria are close to the nuclear envelope along the concave side while the fibrous pericentriolar structure is located along the convex side of the nucleus (Fig. 3a).

As the advanced spermatid develops further the nucleus adopts a more open “C” shape (Fig. 3b, c). In the final stages of development, the spermatid’s mitochondria distribute in two groups one at each end of the concave side of the nucleus (Fig. 3c). Two centrioles aligned in parallel can be observed in the convex

side somewhat displaced from its centre. Each of them exhibits the typical cylindrical structure consisting of 9 triplets of microtubules (Fig. 3c).

Ultrastructure of the spermatozoon

The spermatozoon of *L. crocodilus* is a biflagellate cell with a long and curved conical-shaped head of about 6 μm , a short neck, and two long flagella of 55 μm (Fig. 1c, d). Due to the form of the spermatozoon head, the following morphological regions can be established: an anterior end, a posterior end, a concave side (which arises from the apical pole of the spermatid) and a convex side (derived from the basal pole of the spermatid) (Fig. 1d). The posterior end of the head is wider than the anterior end, which looks like a cylindrical appendix (Fig. 1d). The nucleus occupies practically the whole volume of the head and shows the same elongated and curved conformation (Fig. 3d).

Two sets of mitochondria, one at each end of the head, are present. They are small and with few cristae and are close to the nuclear envelope of the concave side (Fig. 3d, e). At the convex side and in close proximity to the posterior end, the cytoplasm expands slightly to form a short neck where the two centrioles align in parallel, adopting an orientation of about 60° with respect to the nuclear surface (Fig. 3f, g). The distal ends of both centrioles are oriented towards the posterior end of the spermatozoon, where the axonemes of the flagella emerge (Fig. 3f, g). The fibrous pericentriolar structure that was already apparent in the spermatid can also be observed in the spermatozoon neck at the cytoplasmic region between the nuclear envelope and the proximal end of both centrioles (Fig. 3f).

The axonemes of both flagella do not exhibit the canonical 9+2 pattern. Instead they display the 9+0 pattern as they only contain the nine peripheral microtubule doublets (Fig. 3h). The diameter of the flagellum is ~250 nm. However, sections of smaller diameter (~200 nm) corresponding to the distal end of the flagellum and showing one of the doublets displaced to the centre can also be observed (Fig. 3h, arrow).

Chromatin condensation pattern and characterization of the SNBPs

Fig. 4 summarizes the chromatin condensation pattern observed during the spermiogenesis of *L. crocodilus*. At the early spermatid stages chromatin has a fibrogranular appearance with granules of 25 ± 5 nm in diameter. Condensation of the chromatin takes place starting from the nuclear periphery with the appearance of granular structures of 50 ± 5 nm that gradually replace the 25 ± 5 nm organization, which can still be observed in the centre of the nucleus (Fig. 4a). The nucleus is voluminous and round at this stage (Figs. 2a, b). During the transition to middle spermatid the nucleus not only begins to lose its spherical conformation but its chromatin undergoes a progressive condensation into larger globular structures of 150 ± 50 nm in diameter (Fig. 4b, see also Fig. 2g). These will progressively coalesce through the stage of advanced spermatid, giving rise to a highly condensed chromatin organization (Fig 4c, Fig. 3a,b,c) similar to that finally observed in the spermatozoon (Fig. 3e, g).

The biochemical characterization of the proteins associated with this highly condensed chromatin was investigated. Fig. 5a shows the electrophoretic pattern of the proteins extracted with 0.4 N HCl from the nuclei of sperm and ripe testis

from *L. crocodilus*. For comparison purposes, histones (from chicken erythrocyte) and salmine (salmon protamine) are also shown. In both the sperm and the testis extracts, the protein bands appear distributed in two major regions according to their electrophoretic mobility: several protein bands that migrate in the histone region and a group of faster migrating electrophoretic bands (P in Fig. 5a) with a mobility intermediate between histones and salmine. The latter group consists of three proteins, P1, P2 and P3, which are quantitatively the most important of the extract.

To further characterize the SNBPs of *L. crocodilus*, a sequential acid solubilisation of these proteins was carried out (Fig. 5b). The sperm nuclei from ripe testes of *L. crocodilus* were divided into two aliquots. The first nuclei aliquot was used to perform a 0.4 N HCl extract as before (HCl in Fig. 5b), while the second aliquot was first extracted with 35% acetic acid (AC) and then reextracted with 0.4 N HCl (post acetic acid extraction) (PA) (Fig. 5b). Both linker (H1 family) and core histones (H2A, H2B, H3, H4) are typically extracted with 35% acetic acid (Subirana et al. 1973; Saperas et al. 1993a), while proteins with a higher arginine/lysine ratio such as protamines require stronger acids (0.4 N HCl) for their complete extraction. Although some other minor bands can be detected, the AC extract from *L. crocodilus* sperm nuclei consists mainly of histone proteins. This can be clearly ascertained from the two-dimensional gel as shown by their electrophoretic migration in the SDS-PAGE second dimension (Fig. 5c, AC). However, the faster migrating P fraction as well as some proteins that migrate in the histone mobility region are mostly found in the PA extract (see arrows in Fig. 5b). This is indicative of a higher basicity of these proteins. Furthermore, the fact that these same proteins do not enter into the SDS gel of the 2D-PAGE (arrows in

Fig. 5c) strongly indicates that these proteins must be arginine-rich (Chiva and Subirana 1987; Chiva et al. 1990; Saperas et al. 1993a).

Although in AU-PAGE the faster P fraction does not exhibit the high electrophoretic mobility which is characteristic of fish protamines (see lane S in Fig. 5a), the biochemical behaviour of these proteins during the acid extractions and in the 2D-PAGE suggests that the proteins present in this fraction (P1, P2 and P3) could be considered as protamines. Characterization of the HCl, AC and PA acid extracts was carried out by RP-HPLC (Fig. 6a, b). The electrophoretic analysis (Fig. 6b) reveals how the P fraction of *L. crocodilus* SNBPs corresponds to the first proteins to elute in this chromatography, as it would be expected from highly hydrophilic molecules. By contrast, when cationic exchange-FPLC was used to fractionate the same extracts, these proteins were the last to elute and required high concentrations of NaCl (from 1.6 M up to 2 M NaCl), as it would be expected from highly positively proteins which bind with higher strength in this type of chromatography. None of the gradients assayed with both types of columns nor the HPLC repurification of the FPLC purified samples allowed us to obtain the three proteins as separated peaks. However, selection of the best fractions from several of the chromatographies allowed us to carry out a preliminary amino acid analysis from protein fractions P1 and P3 (see Fig. 6e and Table 1). Also the molecular mass of P1, P2 and P3 proteins could be determined by mass spectrometry (Fig. 6d).

Table 1 shows the amino acid composition and molecular mass of P1 and P3 from *L. crocodilus* compared to those of several fish and other vertebrate protamines. The amino acid analyses reveal that the basic nature of the P fraction of *L. crocodilus* SNBPs is the result of a high arginine content (42.2 mol percent and

46.2 mol percent for P1 and P3 fractions, respectively), which is highly characteristic of protamines, being the content of lysine much lower (4.4 mol percent and 3.5 mol percent, respectively). As with protamines, the content of the phosphorylatable amino acids serine+threonine is also significantly high. Mass spectrometry analysis of *L. crocodilus* protamines estimates the molecular mass of the proteins in the P fraction (10211 Da, 9770 Da and 9484 Da for P1, P2 and P3, respectively) (Fig. 6d). These values are much higher than the typically observed for other fish protamines (usually between 4000 Da and 5000 Da) (Table 1).

Discussion

Ultrastructural studies

Our observations of the early spermatid of *L. crocodilus* agree essentially with those of Mattei and Mattei (1976). Thus, we also observe in this stage a voluminous central nucleus; the existence of two parallel centrioles that give rise to two flagella of the 9+0 type (still short at this stage); and the presence of a dense fibrous pericentriolar formation. However, we add some more observations on the early spermatid, such as the chromatin organization (discussed below), or the perinuclear disposition of the mitochondria at this stage (that will be lost later on). We also show how this spermatid develops into the spermatozoon.

According to Mattei et al. (1978) we observe that the liberation of cytoplasmic drops takes place from the early stages of spermiogenesis, without the active participation of the Sertoli cells. They do participate, however, in the phagocytosis of these residual bodies. Thus Sertoli cells with a high number of lysosomes are observed in the walls of the spermatogenic tubules (Fig. 2d). Also, the fact that a mix of spermatids and sperm cells can be seen in the lumen of the spermatogenic tubules (Fig. 2a, b) is an indication that spermatogenesis could be of the semi-cystic type in this species.

The changes in the nucleus morphology, from spherical to the final curved conical-shape, are accompanied by an enlargement of the fibrous pericentriolar structure, which progressively extends through the basal pole of the nucleus. An electron dense plate is also described in the monoflagellate and biflagellate spermatozoa of the family Apogonidae (cardinal fish) (Lahnsteiner 2003; Fishelson et al. 2006).

The precise function and composition of this fibrous structure is not known. It could be constituted by microtubules or by fibrillar proteins other than tubulin. In *L. crocodilus* this fibrous pericentriolar structure found along the convex side of the nucleus could be involved in the nuclear morphogenesis process, playing a role in the remodelling of the nuclear (and the sperm head) shape; it could also be involved in the anchoring of the centrioles. Other possibilities such as a role in the fertilization process cannot be excluded (note in Fig. 3a how FS protrudes forward resembling the cylindrical appendix found in the anterior end of the spermatozoon head shown in Fig. 1d).

At the same time a reorganization of the chondriome is observed and the size and number of mitochondria are reduced. During spermiogenesis, mitochondria usually move towards the basal pole of the cell, where the flagellum is found. Instead, in *L. crocodilus*, mitochondria move far away from the centrioles, to be finally found at both ends of the concave side and close to the nuclear envelope in the spermatozoon (see Fig. 2a, e, 3a, d, and the detail in Fig 3e). In the Myctophidae *Symbolophorus californiensis* and *Notoscopelus* sp., small spherical mitochondria are also found in the concave side in close contact with the nuclear membrane. However, according to Hara (2007), they are numerous and distributed along all the length of the nucleus. A similar event is observed in Elopomorpha fishes, which also presents an elongated sperm nucleus. In this group, mitochondria migrate during spermiogenesis to settle frequently at the tip of the nucleus opposite the end at which the centrioles are located. However, only one mitochondrion is found in this case, as mitochondria fuse into a single structure. The flagellum is also of the 9+0 pattern, but it is located perpendicular to the elongated nucleus. Another difference is that the proximal centriole of the

Elopomorpha is extended as two elongate bundles of 4 and 5 triplets running towards the tip of the elongate nucleus, which may extend as a pseudoflagellum (Mattei 1991a, 1991b; reviewed in Jamieson 1991, Jamieson and Mattei 2009). Instead *L. crocodilus* presents biflagellarity.

While uniflagellate spermatozoa are mostly observed in fishes, biflagellarity has been reported in some species of the orders Polypteriformes (bichirs) (Mattei 1970), Ceratodontiformes (lungfishes) (Boisson et al. 1967; Mattei 1970; Pukerson et al. 1974), and four orders among teleost fishes: Siluriformes (catfishes) (Jamieson 1991, 2009a; Shain 2006; Spadella et al. 2006; Quagio-Grassiotto et al. 2011), Myctophiformes (lanternfishes) (Mattei and Mattei 1976, Hara 2007), Batrachoidiformes (toadfishes) (Hoffman 1963; Casas et al. 1981; Stanley 1965), and Perciformes (Mattei and Mattei 1978, 1984; Yao et al. 1995; Mattos et al. 2002; Lahnsteiner 2003; Fishelson et al. 2006) (more details can be found in Jamieson 2009b). Uniflagellate and biflagellate species can be found sometimes in the same order and even in the same family. For instance, among Ceratodontiformes, *Protopterus* (African lungfish, Proptopteridae) is biflagellate (Boisson et al. 1967; Mattei 1970; Pukerson et al. 1974) while *Neoceratodus* (Australian lungfish, Ceratodontidae) has one flagellum (Jespersen 1971); in Siluriformes, there are families such as Cetopsidae, Aspredinidae, Nematogenyidae or Malapteruridae that are biflagellate, while others like Pimelodidae, Diplomystidae, Siluridae or Clariidae are uniflagellate (Jamieson 1991, 2009a; Shain 2006; Spadella et al. 2006; Quagio-Grassiotto et al. 2011). Both uniflagellate and biflagellate species have been reported in the family Doradidae (Siluriformes) (Quagio-Grassiotto et al. 2011). It is also remarkable that in Apogonidae (Perciformes), sperm with one or two flagella can be found in a

same species, percentage of each type differing in males of different lengths, as well as in different species (Fishelson et al. 2006).

Among Myctophiformes, *Lampanyctodes hectoris* and *Diaphus danae* are said to have aflagellate sperm (Young et al. 1987), although this statement needs confirmation (see also Jamieson 1991, pp. 159-160). Thus Myctophidae could include aflagellate, uniflagellate and biflagellate sperm, although it has to be ascertained whether this diversity of sperm structure indicates polyhyly (Jamieson 2009b). In this sense, it would be very interesting to study the sperm cells of more myctophiform species.

Until now, Elopomorpha is the only other group of fishes with the 9+0 axoneme pattern. No phylogenetic significance can be attached to these resemblances to *Lampanyctus* nor is their functional significance clear (Jamieson 1991).

Thus, to our knowledge, and as already stated by Mattei and Mattei (1976), Myctophidae is the only group of fishes where biflagellarity and the 9+0 axoneme structure have been found to coexist.

Note: All the fish species and groups mentioned follow Nelson's (2006) classification.

SNBPs and chromatin condensation

Although some amount of histones and other basic proteins of similar electrophoretic mobility are found in the sperm cell of *L. crocodilus*, the main SNBPs found in this species are proteins P1, P2 and P3. The compositional analysis of almost pure fractions of P1 and P3 (Table 1) shows that they can be classified as protamines. They have a high content of basic amino acids (around 50 mol%) mainly constituted by arginine, very low presence (if any) of acidic and aromatic amino acids, and the presence of phosphorylatable amino acids (serine and threonine). The only differing trend is the amount of alanine, which is higher than usual. One of the typical characteristics of protamines is that arginines are found associated in clusters. Although not easy to do, it would be very interesting to sequence these proteins to verify if the high amount of arginine that they present is also organized in clusters.

L. crocodilus protamines, however, differ from the other known fish protamines in their size. Fish protamines are typically small proteins, usually constituted by 30-40 amino acids, with molecular masses around 4000 and 5000 Da. Although there are some cases of somewhat bigger protamines in fishes (among the Gasterosteiformes and the Scorpaeniformes) (Giménez-Bonafé et al. 2000; Frehlick et al. 2006), they are no larger than 6700 Da (Table 1). In contrast, *L. crocodilus* protamines present estimated molecular masses of 9500-10200 Da (Fig. 6d), about double the value of most fish protamines and closer to birds' protamines (Table 1). In the case of birds it has been suggested that the presence of some internal homologies in the *Gallus* protamine sequence and its increased length compared to fish protamines might be due to a partial duplication event during the evolution of birds (Dixon et al. 1985). We do not know at present if a

gene duplication could be involved in the case of *L. crocodilus*. Another possibility would be that proteins in the P fraction of *L. crocodilus* corresponded to especially arginine-enriched PL-type proteins such as that found in *Chaetopterus variopedatus* (De Petrocellis et al. 1983; Piscopo et al. 1993; Fioretti et al. 2012).

One common feature observed during the initial stages of spermiogenesis in several species is the disappearance of the structural differences between euchromatin and heterochromatin, with a nuclear chromatin organization consisting of uniformly distributed 20 nm granules (Ribes et al. 2001; Kurtz et al. 2009; Chiva et al. 2011). In a previous study, it has been proposed that this can be considered to be the ancestral model of nuclear differentiation in animal spermiogenesis (Kurtz et al. 2009). According to this work, histones are partially acetylated during the early stages of spermiogenesis, resulting into a homogeneous chromatin structure consisting of 20 nm granules that can be observed in a number of species. In the most simple cases, histones are later deacetylated, leading to a certain degree of chromatin condensation. This is, for instance, the case for the fish *Sparus aurata*, which has the H-type SNBPs (Kurtz et al. 2009). In more advanced cases, protamines displace the acetylated histones leading to a much higher degree of chromatin condensation. In the fish *Dicentrarchus labrax*, where a canonical fish protamine of 34 amino acids replaces histones during spermiogenesis (Saperas et al. 1993b), granules of about 20 nm can be observed in the earlier stages. However, as spermiogenesis progresses, these granules undergo a chromatin remodelling into progressively larger coarse granules of about 80 nm, concomitantly with substitution of histones by

protamines. Finally these coarse granules coalesce resulting in an almost uniformly packaged chromatin (Kurtz et al. 2009).

In the case of *L. crocodilus* a similar simple condensation pattern is observed starting with 25 nm fibrogranular structures, which would be equivalent to those described above for other species. Progressively, granules of about 50 ± 5 nm and 150 ± 50 nm develop, which finally coalesce to produce the highly condensed chromatin observed in the sperm cell. Although we do not have direct experimental evidence, most probably the final 150 ± 50 nm granules are constituted by protamine-associated DNA. The presence of intermediate sized granules is likely related to the fact that *L. crocodilus* SNBPs do not exclusively consist of protamines but also of a certain amount of histones and other more basic proteins. The fusion of the coarse granules observed in the final stages of spermiogenesis in this work, as well as in a number of species is probably related to protamine dephosphorylation (Kurtz et al. 2009; Chiva et al. 2011). It has been described by several authors (Oliva and Dixon 1991; Lewis et al. 2003; Martínez-Soler et al. 2007) that protamines are phosphorylated at the time when they replace histones and they are subsequently dephosphorylated during the final stages of spermiogenesis. This enhances protein-DNA interaction producing the homogeneous (or quasi-homogeneous) chromatin of the sperm cell.

In conclusion, in the fish *Lampanyctus crocodilus* (Myctophiformes, Myctophidae) a number of particularities converge: the presence of a biflagellate spermatozoon, the 9+0 axoneme pattern, an unusual redistribution of mitochondria during spermiogenesis, and the presence of the largest protamines known to date in

fishes. It would be very interesting to investigate more myctophiform species to check how widespread these characteristics are within the group (especially with regard to the number and type of flagella).

Acknowledgements

We are very grateful to José Antonio Caparrós and the crew of the fishing boats *Nus* and *l'Òstia* for kindly providing us with the biological material. We are also thankful to Raquel Sánchez-Giraldo for her help with sample transportation and for her assistance with the FPLC, as well as Enric Huguet and Sara K. Murase for their help with the translation from Japanese. Microscopic observations were performed in the Scientific Technical Services of the University of Barcelona. This work was supported in part by Fundació Bosch i Gimpera (Universitat de Barcelona) to E.R., by grant BFU2009-10380 (Ministerio de Ciencia e Innovación, Spain), FEDER, and AQU-2009-SGR-1208 (Generalitat de Catalunya) to N.S., and by a Natural Sciences and Engineering Research Council of Canada (NSERC) 46399-2012 grant to J.A.

References

- Ando T, Watanabe S (1969) A new method for fractionation of protamines and the amino acid sequence of one component of salmine and three components of iridine. *Int J Protein Res* 1:221-224
- Ausió J (1988) An unusual cysteine-containing histone H1-like protein and two protamine-like proteins are the major nuclear proteins of the sperm of the bivalve mollusc *Macoma nasuta*. *J Biol Chem* 263: 10141-10150
- Ausió J (1999) Histone H1 and evolution of sperm nuclear basic proteins. *J Biol Chem* 274:31115-31118
- Boisson C, Mattei X, Mattei C (1967) Troisième note sur la spermiogenèse de *Protopterus annectens* (Dipneuste) du Sénégal. Institut Fondamental d'Afrique Noire. Bulletin série A (Sciences Naturelles) 29:1097-1121
- Buesa C, del Valle L, Saperas N, Goethals M, Lloris D, Chiva M (1998) Primary structure of scombrine α : two different species with an identical protamine. *Comp Biochem Physiol* 119B:145-149
- Casas MT, Muñoz-Guerra S, Subirana JA (1981) Preliminary report on the ultrastructure of chromatin in the histone containing spermatozoa of a teleost fish. *Biol Cell* 40:87-92
- Chiva M, Kasinsky HE, Mann M, Subirana JA (1988) On the diversity of sperm basic proteins in the vertebrates. VI. Cytochemical and biochemical analysis in birds. *J Exp Zool* 245:304-317
- Chiva M, Lafargue F, Rosenberg E, Kasinsky HE (1992) Protamines, not histones, are the predominant basic proteins in sperm nuclei of solitary ascidian tunicates. *J Exp Zool* 263:338-349
- Chiva M, Rosenberg E, Kasinsky HE (1990) Nuclear basic proteins in mature testis of the ascidian tunicate *Styela montereyensis*. *J Exp Zool* 253:7-19
- Chiva M, Saperas N, Ribes E (2011) Complex chromatin condensation patterns and nuclear protein transitions during spermiogenesis: Examples from mollusks. *Tissue Cell* 43:367-376
- Chiva M, Subirana JA (1987) Mètode per a obtenir protamines testiculars riques en arginina. IV Jornades de Biologia Molecular (Societat Catalana de Biologia), pp 77-80
- Daban M, Martinage A, Kouach M, Chiva M, Subirana JA, Sautière P (1995) Sequence analysis and structural features of the largest known protamine isolated from the sperm of the archaeogastropod *Monodonta turbinata*. *J Mol Evol* 40:663-670

- De Petrocellis B, Parente A, Tomei L, Geraci G (1983) An H1 histone and a protamine molecule organize the sperm chromatin of the marine worm *Chaetopeterus variopedatus*. *Cell Differ.* 12:129-135.
- Dixon GH, Aiken JM, Jankowski JM, McKenzie DI, Moir R, States JC (1985) Organization and evolution of the protamine genes of salmonid fishes. In: Reek G, Goodwin G, Puigdomènech P (eds) *Chromosomal proteins and gene expression*. Plenum Press, New York, pp 287-314
- Eirín-López JM, Ausió J (2009) Origin and evolution of chromosomal sperm proteins. *Bioessays* 31:1062-1070
- Fioretti FM, Febbraio F, Carbone A, Branno M, Carratore V, Fucci L, Ausió J, Piscopo M (2012) A sperm nuclear basic protein from the sperm of the marine worm *Chaetopterus variopedatus* with sequence similarity to the arginine-rich C-termini of chordate protamine-likes. *DNA Cell Biol.* 31:1392-402
- Fishelson L, Delarea Y, Gon O (2006) Testis structure, spermatogenesis, spermatocytogenesis, and sperm structure in cardinal fish (Apogonidae, Perciformes). *Anat Embryol* 211:31-46
- Frehlick LJ, Eirín-López JM, Prado A, Su HW, Kasinsky HE, Ausió J (2006) Sperm nuclear basic proteins of two closely related species of scorpaeniform fish (*Sebastes maliger*, *Sebastes* sp.) with different sexual reproduction and the evolution of fish protamines. *J Exp Zool* 305A:277-287
- Giménez-Bonafé P, Laszczak M, Kasinsky HE, Lemke MJ, Lewis JD, Iskandar M, He T, Ikonomou MG, White FM, Hunt DF, Chiva M, Ausió J (2000) Characterization and evolutionary relevance of the sperm nuclear basic proteins from stickleback fish. *Mol Reprod Dev* 57:185-193
- Hara M (2007) Ultrastructure of spermatozoa of two species of Myctophidae; *Symbolophorus californiensis* and *Notoscopelus* sp. *Japan J Ichthyol* 54:41-46
- Hara M, Okiyama M (1998) An ultrastructural review on the spermatozoa of Japanese fishes. *Bulletin of the Ocean Research Institute, University of Tokyo* 33:1-138
- Hoffman RA (1963) Gonads, spermatid ducts, and spermatogenesis in the reproductive system of male toadfish, *Opsanus tau*. *Chesapeake Science* 4:21-29
- Hulley PA (1984) Myctophidae. In: Whitehead PJP, Bauchot ML, Hureau JC, Nielsen J, Tortonese E (eds) *Fishes of the North-eastern Atlantic and the Mediterranean (FNAM)*. UNESCO, Paris, vol I, pp 429-483
- Hunt JG, Kasinsky HE, Elsey RM, Wright CL, Rice P, Bell JE, Sharp DJ, Kiss AJ, Hunt DF, Arnott DP, Russ MM, Shabanowitz J, Ausió J (1996) Protamines of reptiles. *J Biol Chem* 271:23547-23557
- Jamieson BGM (1991) *Fish evolution and systematics: Evidence from spermatozoa*. Cambridge University Press, Cambridge

- Jamieson BGM (2009a) Reproductive biology and phylogeny of fishes (agnathans and bony fishes): phylogeny, reproductive system, viviparity, spermatozoa. Jamieson BGM (ed) Reproductive biology and phylogeny series, vol 8, part A, Science Publishers, Enfield (NH), pp. 1-788
- Jamieson BGM (2009b) Ultrastructure of spermatozoa: Neoteleostei: Stenopterygii, Cyclosquamata, Scopelomorpha and Paracanthopterygii. In: Reproductive biology and phylogeny of fishes (agnathans and bony fishes): phylogeny, reproductive system, viviparity, spermatozoa. Jamieson BGM (ed) Reproductive biology and phylogeny series, vol 8, part A, Science Publishers, Enfield (NH), pp 415-445
- Jamieson BGM, Mattei X (2009) Ultrastructure of spermatozoa: Elopomorpha and Clupeomorpha. In: Reproductive biology and phylogeny of fishes (agnathans and bony fishes): phylogeny, reproductive system, viviparity, spermatozoa. Jamieson BGM (ed) Reproductive biology and phylogeny series, vol 8, part A, Science Publishers, Enfield (NH), pp 255-285
- Jespersen Å (1971) Fine structure of the spermatozoon of the Australian lungfish *Neoceratodus forsteri* (Krefft). J Ultrastr Res 37:178-185
- Kasinsky HE, Frehlick LJ, Su HW, Ausió J (2005) Protamines in the internally fertilizing neobatrachian frog *Eleutherodactylus coqui*. Mol Reprod Dev 70:373-381
- Kurtz K, Saperas N, Ausió J, Chiva M (2009) Spermiogenic nuclear protein transitions and chromatin condensation. Proposal for an ancestral model of nuclear spermiogenesis. J Exp Zool (Mol Dev Evol) 312B:149-163
- Laemmli UK (1970) Cleavage of structural proteins during the assembly of the head of the bacteriophage T4. Nature 227:680-685
- Lahnsteiner F (2003) The spermatozoa and eggs of the cardinal fish. J Fish Biol 62:115-128
- Lahnsteiner F, Patzner RA (2007) Sperm morphology and ultrastructure in fish. In: Alavi SMH, Cosson JJ, Coward K, Rafiee G (eds) Fish spermatology. Alpha Science International Ltd, Oxford, pp 1-61
- Lewis J, Song Y, de Jong M, Bagha S, Ausió J (2003) A walk through vertebrate and invertebrate protamines. Chromosoma 111:473-482
- Martínez-Soler F, Kurtz K, Ausió J, Chiva M (2007) Transition of nuclear proteins and chromatin structure in spermiogenesis of *Sepia officinalis*. Mol Reprod Dev 74:360-370
- Mattei C, Mattei X (1978) La spermiogenèse d'un poisson téléostéen (*Lepadogaster lepadogaster*). II-Le spermatozoïde. Biologie Cellulaire 32:267-274
- Mattei C, Mattei X (1984) Spermatozoïdes biflagellés chez un poisson téléostéen de la famille Apogonidae. J Ultrastr Res 88:223-228

- Mattei C, Mattei X, Marchand B (1978) Elimination de cytoplasme par les spermatozoïdes jeunes de deux poissons téléostéens: *Citharinus* sp. et *Lampanyctus* sp. C R Soc Biol 172:393-396
- Mattei X (1970) Spermiogenèse comparée des poissons. In: Baccetti B (ed) Comparative Spermatology. Academic Press, New York, pp 57-69
- Mattei X (1991a) Spermatozoon ultrastructure and taxonomy in fishes. In: Baccetti B (ed) Proceeding of the VIth International Congress on Spermatology, Siena. Raven Press, New York, pp 985-990
- Mattei X (1991b) Spermatozoon ultrastructure and its systematic implications in fishes. Can J Zool 69:3038-3055
- Mattei X, Mattei C (1976) Spermatozoïdes à deux flagelles de type 9+0 chez *Lampanyctus* sp. (poisson Myctophidae). J Microsc Biol Cell 25:187-188
- Mattos E, Santos MNS, Azevedo C (2002) Biflagellate spermatozoon structure of the hermaphrodite fish *Satanoperca jurupari* (Heckel, 1840) (Teleostei, Cichlidae) from the Amazon river. Braz J Biol 62:847-852
- Nelson JS (2006) Fishes of the world. 4th edition. John Wiley & Sons, Hoboken, NJ
- Okamoto Y, Muta E, Ota S (1987) Primary structures of M6 and M7 of mugiline beta (*Mugil japonicus*). J Biochem 101:1017-1024
- Oliva R, Dixon GH (1989) Chicken protamine genes are intronless. The complete genomic sequence and organization of the two loci. J Biol Chem 264:12472-12481
- Oliva R, Dixon GH (1991) Vertebrate protamine genes and the histone-to-protamine replacement reaction. Prog. Nucleic Acid Res. Mol. Biol. 40:25-94
- Puckerson ML, Jarvis JUM, Luse SA, Dempsey EW (1974) X-ray analysis coupled with scanning and transmission electron microscopic observations of spermatozoa of the African lungfish, *Protopterus aethiopicus*. J Zool (London) 172:1-12
- Piscopo M, Tomei L, De Petrocellis L, Geraci G (1993) Anion-mediated lysine-arginine interaction. Evidence in *Chaetopterus variopedatus* sperm protamine. FEBS Lett. 334:125-127.
- Quagio-Grassiotto I, Ortiz RJ, Sabaj Pérez MH, Oliveira C (2011) Sperm of Doradidae (Teleostei: Siluriformes) Tissue Cell 43:8-23
- Ribes E, Sánchez de Romero LD, Kasinsky HE, del Valle L, Giménez-Bonafé P, Chiva M (2001) Chromatin reorganization during spermiogenesis of the mollusk *Thais hemostoma* (Muricidae). Implications for sperm nuclear morphogenesis in cenogastropods. J Exp Zool 289:304-316

- Saperas N, Ausió J, Lloris D, Chiva M (1994) On the evolution of protamines in bony fish: Alternatives to the “retroviral horizontal transmission” hypothesis. *J Mol Evol* 39:282-295
- Saperas N, Chiva M, Ausió J (1992) Purification and characterization of the protamines and related proteins from the sperm of a tunicate, *Styela plicata*. *Comp Biochem Physiol B* 103:969-974
- Saperas N, Lloris D, Chiva M (1993a) Sporadic appearance of histones, histone-like proteins, and protamines in sperm chromatin of bony fish. *J Exp Zool* 265:575-586
- Saperas N, Ribes E, Buesa C, García-Hegart F, Chiva M (1993b) Differences in chromatin condensation during spermiogenesis in two species of fish with distinct protamines. *J Exp Zool* 265:185-194
- Shain AAB (2006) Semicystic spermatogenesis and biflagellate spermatozoon ultrastructure in the Nile electric catfish *Malapterus electricus* (Teleostei: Siluriformes: Malapteruridae) *Acta Zoologica* 87:215-227
- Spadella MA, Oliveira C, Quagio-Grassiotto I (2006) Occurrence of biflagellate spermatozoa in Cetopsidae, Aspredinidae, and Nematogenyidae (Teleostei: Ostariophysi: Siluriformes) *Zoomorphology* 125:135-145
- Stanley HP (1965) Electron microscopic observations on the biflagellate spermatids of the teleost fish *Porichthys notatus*. *Anatomical Record* 151:477
- Subirana JA, Cozcolluela C, Palau J, Unzeta M (1973) Protamines and other basic proteins from spermatozoa of molluscs. *Biochim Biophys Acta* 317:364-379
- Suzuki K, Ando T (1972) Studies on protamines. XVII. The complete amino acid sequence of clupeine YI. *J Biochem* 72:1433-1446
- Takamune K, Nishida H, Takai M, Katagiri C (1991) Primary structure of toad sperm protamines and nucleotide sequence of their cDNAs. *Eur J Biochem* 196:401-406
- Young JW, Blaber SJM, Rose R (1987) Reproductive biology of three species of midwater fishes associated with continental slope of eastern Tasmania, Australia. *Marine Biology* 95:323-332
- Yao Z, Emerson CJ, Crim LW (1995) Ultrastructure of the spermatozoa and eggs of the ocean pout (*Macrozoarces americanus* L.), an internally fertilizing marine fish. *Mol Reprod Dev* 42:58-64
- Yulikova EP, Rybin VK, Silaev AB (1979) The primary structure of stellin A. *Bioorg. Khim.* 5:5-10

Figure legends

Fig. 1 Scanning electron micrographs (SEM) of the spermatid and spermatozoon of *Lampanyctus crocodilus*. **a** General view of the spermatid. **b** View of the head, neck and the two flagella of the spermatid. **c** General view of the spermatozoon. **d** Magnified view of the spermatozoon where the different morphological regions of the head can be identified: anterior end (1), posterior end (2), concave side (3) and convex side (4) (see text for more details). C₁, C₂, centrioles; F₁, F₂, flagella; H, head; Ne, neck. Bars 10 µm (**a,c**), 1 µm (**b, d**).

Fig. 2 Transmission electron micrographs (TEM) of spermatids of *L. crocodilus* at different stages of development. **a, b** Early spermatid. The round nucleus and one of the flagella can be seen. Chromatin presents a fibrogranular appearance. Cisternae of endoplasmic reticulum and mitochondria are observed around the nucleus. The arrowheads point to the fibrous pericentriolar structure. **c** Early spermatid in the process of shedding a large cytoplasmic drop. The arrows indicate residual bodies or cytoplasmic drops produced during the process of spermiogenesis. **d** Image of the spermatogenic tubule wall and lumen. Sertoli cells phagocytosis of the cytoplasmic drops emitted by the spermatids in the lumen of the tubule can be seen. **e** Middle spermatid. The nucleus starts losing its spherical appearance at the apical pole region, while mitochondria start grouping at the nuclear envelope near this area. **f** Detail of the basal region of the middle spermatid. One of the centrioles and the axoneme of one of the flagella can be observed. The pericentriolar structure attached to the nuclear envelope of the basal pole of the nucleus can also be seen. In the nucleus, a large number of

granules of 50 ± 5 nm are observed. **g** Section of a more developed middle spermatid showing granular structures of 150 ± 50 nm in the nucleus. C, centriole; Cd, cytoplasmic drops; ER, endoplasmic reticulum; F, flagellum; FS, fibrous pericentriolar structure; M, mitochondria; MC, peritubular myoid cells; N, nucleus; SC, Sertoli cells; SZ, spermatozoon; V, non-electron dense vesicles. Bars 1 μm (**a-c,e**), 6 μm (**d**), 0.5 μm (**f,g**).

Fig. 3 TEM of the advanced spermatid and spermatozoon of *L. crocodilus*. **a-c** Advanced spermatid. The nuclear morphogenesis transition during spermiogenesis gives rise to a curved conical-shaped nucleus. Mitochondria locate in two groups at both ends of the concave side of the nucleus, while the fibrous pericentriolar structure locates in its convex side. Chromatin appears more condensed due to the agglutination of the 150 ± 50 nm granules. **d-e** Oblique sections at the head level of the spermatozoon. The nucleus occupies most of the spermatozoon head volume and its chromatin shows the same degree of condensation as in the advanced spermatid. Mitochondria are found at both ends of the head. **f-g** Longitudinal sections of the sperm head, neck piece and the two flagella: The fibrous pericentriolar structure can be observed in the neck between the nucleus and the two centrioles, which arrange in parallel at an angle of about 60° with respect to the nucleus. **h** Cross section of the flagella showing the 9+0 doublet axoneme configuration. The arrow indicates the section of a distal end of a flagellum where one of the doublets is displaced to the centre.

C₁, C₂, centrioles; F₁, F₂, flagella; FS, fibrous pericentriolar structure; H, head; M, mitochondria; N, nucleus; Ne, neck; 1-4, as in Fig. 1. Bars 1 μm (**a-d**), 0.5 μm (**e-g**); 200 nm (**h**).

Fig. 4 Chromatin condensation pattern during *L. crocodilus* spermiogenesis (TEM). **a** Early spermatids: Fibrogranular structures of 25 ± 5 nm predominate in the central region and granules of 50 ± 5 nm can be observed in the periphery of the nucleus. **b** Middle spermatid: Chromatin consists mainly of granular structures of 150 ± 50 nm. **c** Advanced spermatid and spermatozoon: The chromatin is much more condensed as a result of the agglutination of the 150 ± 50 nm granules shown in b. Bars 0.2 μ m.

Fig. 5 Electrophoretic analyses of the SNBPs of *L. crocodilus*. **a** AU-PAGE of a 0.4 N HCl sperm (Sp) or ripe testis (T) extract (from one specimen in each case). CM, Chicken erythrocyte histone marker; S, salmine (fish protamine marker from salmon); P, protamines. **b** AU-PAGE of ripe testes acid extracts obtained from several specimens by either direct treatment with 0.4 N HCl, or by sequential 35% acetic acid (AC) and 0.4 N HCl after extraction with 35% acetic acid (PA). Histone H1 and core histones (H2A, H2B, H3, H4) are identified. The arrows on the right side point to the electrophoretic protein bands that do not appear in the second dimension SDS-PAGE shown in (c). **c** Two-dimensional gel electrophoretic analysis of the AC and HCl extracts shown in (b). First dimension (1D) as in (b); second dimension (2D) in SDS-PAGE (15% acrylamide). Arrows as in (b).

Fig. 6 Biochemical characterization of *L. crocodilus* SNBPs. **a** Reversed phase HPLC fractionation of SNBPs extracted with 0.4 N HCl (HCl), 35% acetic acid

(AC), and 0.4 N HCl after extraction with 35% acetic acid (PA) (see Materials and methods for more details). The dotted line corresponds to the acetonitrile elution gradient. P, protamines; CH, core histones. **b** AU-PAGE analysis of some of the fractions collected along the elution profile of the HCl sample shown in (a). The fraction numbers are indicated on top of the gel. HCl, PA and AC, are the same as in (a); CM; chicken erythrocyte marker. **c** FPLC analysis of an HCl extract. The inset shows an AU-PAGE of the proteins of the combined fractions indicated with Roman numerals. The dotted line corresponds to the NaCl elution gradient. **d** Matrix-assisted laser desorption/ionization (MALDI) of fraction 36 in (b) (inset). **e** AU-PAGE of the HPLC and FPLC/HPLC protein fractions used for amino acid analyses (see Table 1).

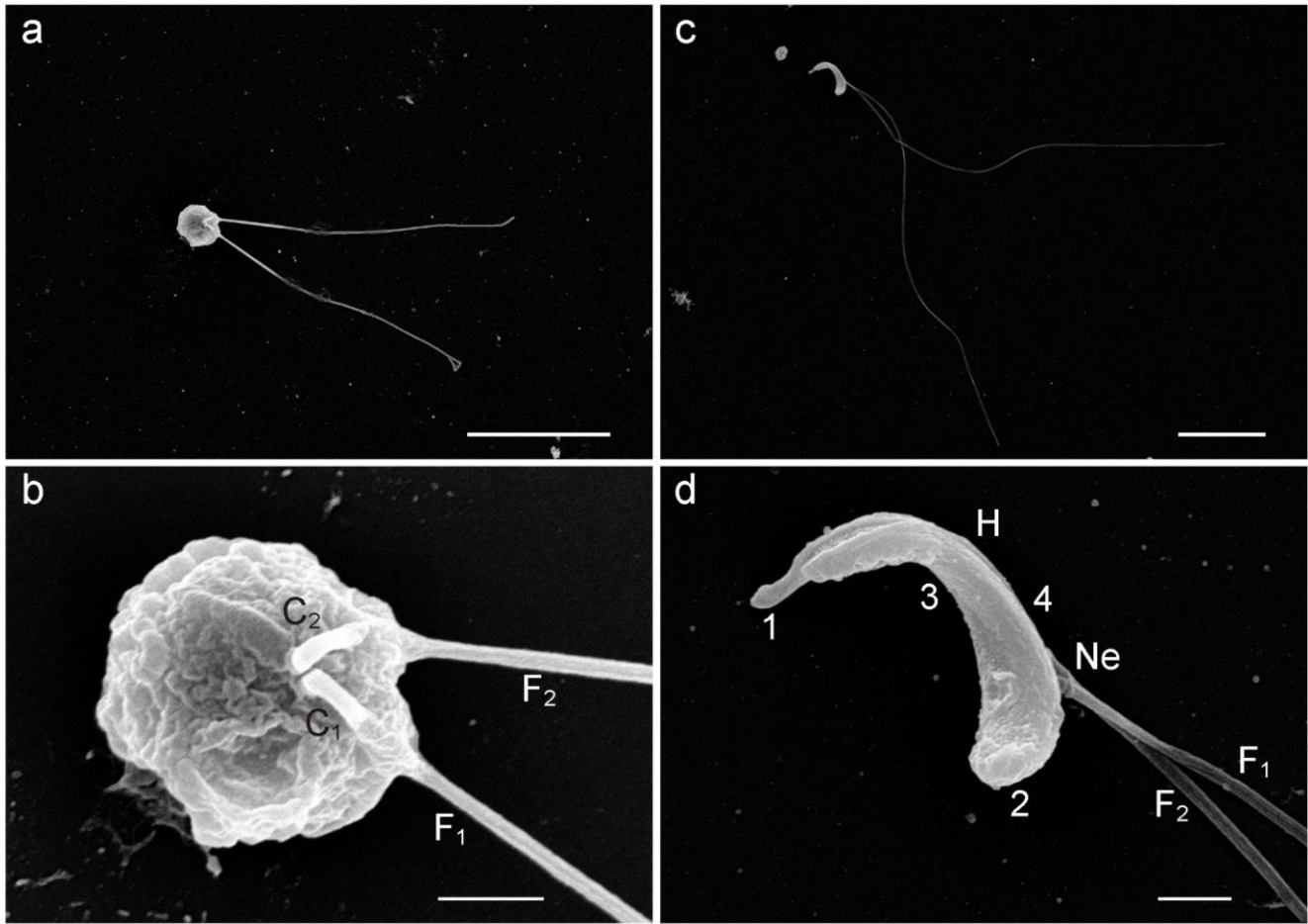


Figure 1

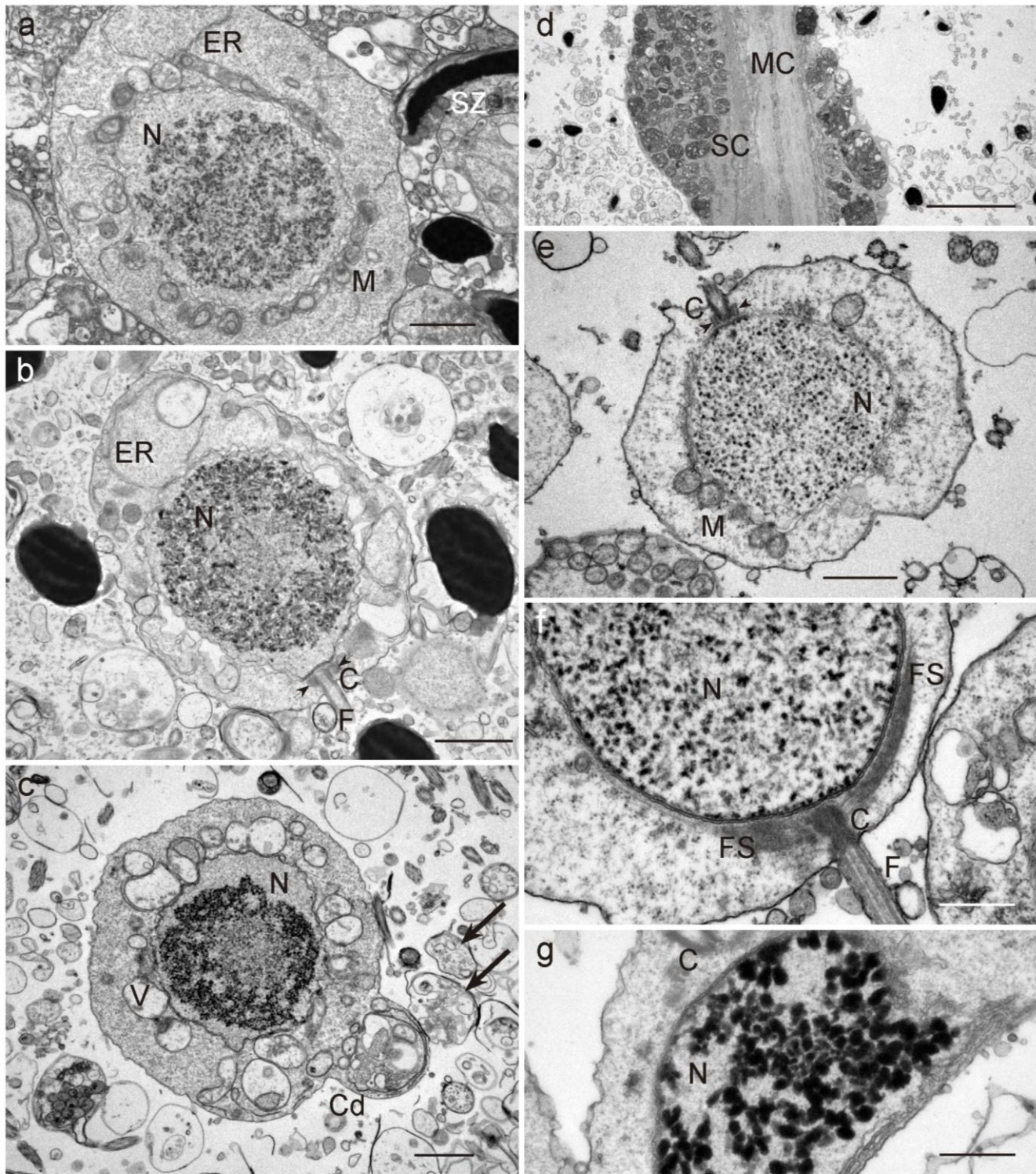


Figure 2

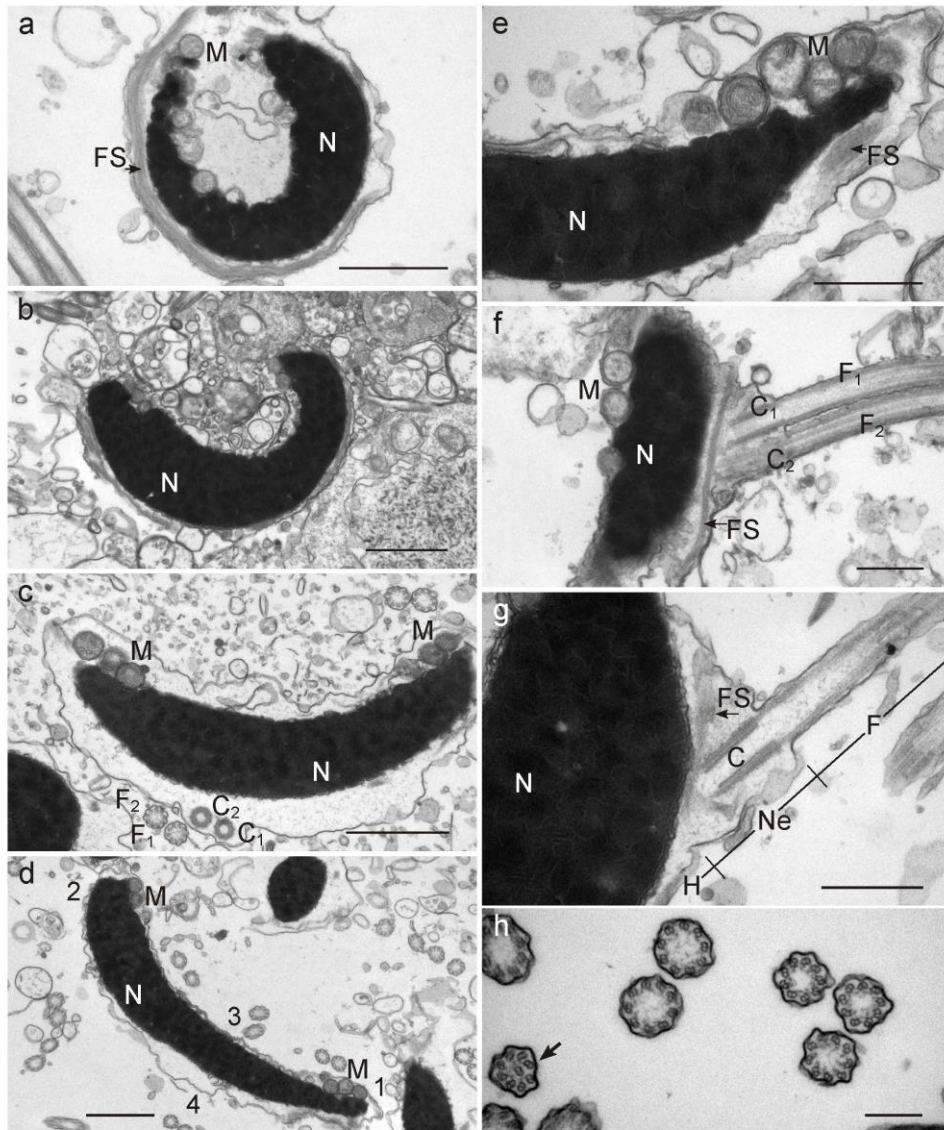


Figure 3

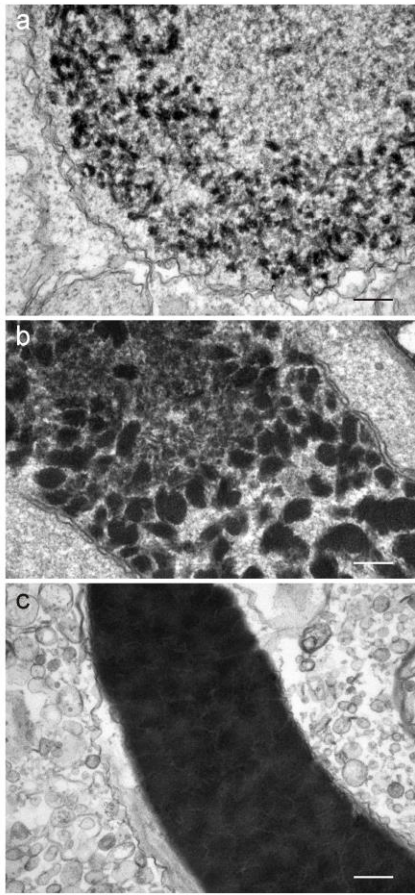


Figure 4

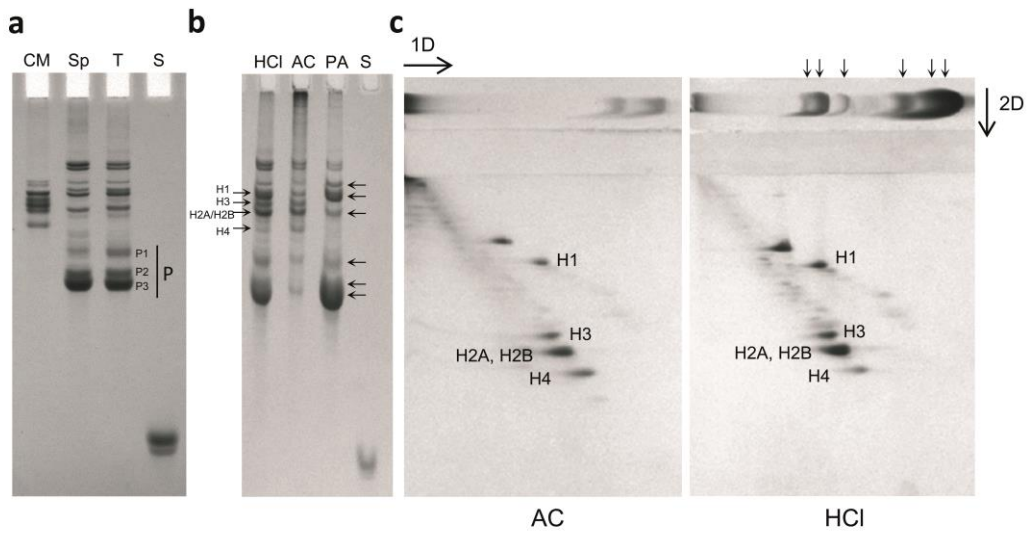


Figure 5

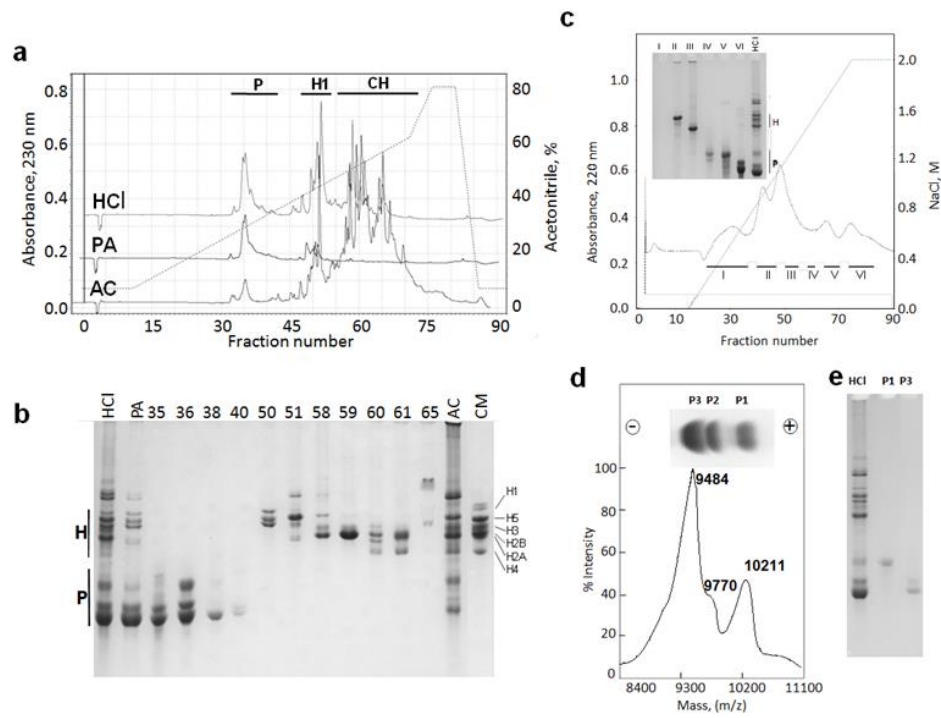


Figure 6

Table 1 Amino acid composition (mol%) of *Lampanyctus crocodilus* protamines (P1 and P3 fractions showed in Fig. 6e) compared to several sequenced protamines from fish and other vertebrate groups.

Amino acid	FISH										AMPHIBIANS	BIRDS
	O. Myctophiformes		O. Acipenseriformes	O. Clupeiformes	O. Salmoniformes	O. Mugiliformes	O. Gasterosteiformes	O. Scorpaeniformes	O. Perciformes			
	<i>Lampanyctus crocodilus</i> ¹		<i>Acipenser stellatus</i>	<i>Clupea pallasii</i>	<i>Onkorhynchus keta</i>	<i>Mugil cephalus</i>	<i>Gasterosteus wheatlandi</i> ⁶	<i>Sebastolobus</i> sp. ⁷	<i>Dicentrarchus labrax</i> ⁸	<i>Scomber scombrus</i>	<i>Bufo japonicus</i>	<i>Gallus domesticus</i> ¹¹
	P1	P3	Stelline A ²	Clupeine YI ³	Salmine AI ⁴	Mugiline β M6 ⁵				Scombrine α ⁹	P1 ¹⁰	
Lys	4.4	3.5	18.5	-	-	-	2.1	3.7	-	-	5.1	-
His	-	-	11.1	-	-	-	2.1	-	-	-	10.3	-
Arg	42.2	46.2	44.4	64.5	65.6	62.5	44.7	48.1	61.8	64.7	43.6	58.1
Asx	0.3	0.3	-	-	-	-	-	1.9 (Asn)	-	-	2.6 (Asp)	-
Thr	7.7	7.1	3.7	6.5	-	3.1	6.4	11.1	5.9	2.9	7.7	1.6
Ser	4.2	3.8	7.4	9.7	12.5	3.1	4.3	5.6	5.9	5.9	5.1	16.1
Glx	1.1	1.2	-	-	-	3.1 (Glu)	2.1 (Gln)	1.9 (Gln)	5.8 (2.9 Glu. 2.9 Gln)	-	2.6 (Gln)	-
Pro	6.4	6.2	-	6.5	9.4	9.4	8.5	5.6	5.9	5.9	10.3	3.2
Gly	2	1.2	3.7	3.2	6.2	-	4.3	3.7	-	-	-	8.1
Ala	21.4	21	7.4	6.5	-	6.2	6.4	9.3	5.9	8.8	5.1	3.2
Cys	-	t	-	-	-	-	-	-	-	-	-	-
Val	8.4	7.6	-	-	6.2	6.2	12.8	7.4	8.8	11.8	5.1	1.6
Met	0.6	0.3	-	-	-	-	-	-	-	-	-	1.6
Ile	0.6	0.9	-	3.2	-	6.2	2.1	-	-	-	-	-
Leu	0.7	0.4	3.7	-	-	-	4.3	1.9	-	-	-	-
Tyr	-	0.3	-	-	-	-	-	-	-	-	2.6	6.5
Phe	-	-	-	-	-	-	-	-	-	-	-	-
Trp	-	-	-	-	-	-	-	-	-	-	-	-
Arg+Lys	46.6	49.7	62.9	64.5	65.6	62.5	46.8	51.8	61.8	64.7	48.7	58.1
Asp+Glu	≤1.4*	≤1.5*	-	-	-	3.1	-	-	2.9	-	-	-
Number of amino acids	u	u	27	31	32	32	47	54	34	34	39	62
Molecular mass (Da)	10211	9484	3532.1	4111.8	4249.9	4317.1	5818.9	6715.8	4565.3	4533.4	5090.8	8117.3

t, traces; u, unknown. (1) This work; (2) Yulikova et al. 1979; (3) Suzuki and Ando 1972; (4) Ando and Watanabe 1969; (5) Okamoto et al. 1987; (6) Giménez-Bonafé et al. 2000; (7) Frehlick et al. 2006; (8) Saperas et al. 1993b; (9) Buesa et al. 1998; (10) Takamune et al. 1991; (11) Oliva and Dixon 1989.

Asx, Asp or Asn; Glx, Glu or Gln; (*) This value could range from 0 (all Asn and Gln) to this maximum value (all Asp and Glu).